Jurnal Sains Materi Indonesia
Indonesian Journal of Materials Science

Vol. 7, No. 3, Juni 2006, hal : 18 - 25
ISSN : 1411-1098

DIELECTRIC PROPERTIES OF SMECTIC-C_α* PHASE

Andika Fajar[1] and Hiroshi Orihara[2]
Technology Center for Nuclear Industrial Materials (PTBIN) - BATAN
Kawasan Puspiptek, Serpong 15314, Tangerang
[2]Division of Applied Physics, Graduate Schoof of Engineering
Hokkaido University, Kita 8 Nishi 5, Sapporo 060-0808, Japan

ABSTRACT

DIELECTRIC PROPERTIES OF SMECTIC-C_α* PHASE. Linear and third-order nonlinear dielectric measurements have been performed within the smectic-C_α* phase of antiferroelectric liquid crystal 4-(1-methyl-heptyloxycarbonyl) phenyl 4-octylcarbonyloxybiphenyl-4-carboxylate (MHPOCBC). In the low temperature region of smectic-C_α* phase, we observed the hysteresis of dielectric constant in cooling and heating process measurement. From the frequency dispersion measurement, it has been found that the frequency relaxation of antiferroelectric Goldstone mode and 'low frequency mode', decreased with increasing the temperature until approach the center of the smectic-C_α* phase.

Key words : Antiferroelectric liquid crystal, nonlinear dielectric constant, MHPOCBC, relaxation mode

ABSTRAK

SIFAT DIELEKTRIK FASA SMEKTIK-C_α*. Telah dilakukan pengukuran dielektrik linier dan order ketiga pada fasa smektik-C_α* dari kristal cair antiferroelectrik 4-(1-methyl-heptyloxycarbonyl) phenyl 4-octylcarbonyloxybiphenyl-4-carboxylate (MHPOCBC). Pada daerah temperatur rendah fasa smektik-C_α*, diamati terjadinya histerisis dari konstanta dielektrik pada pengukuran dengan proses pemanasan dan pendinginan. Dari pengukuran dispersi frekuensi ditemukan bahwa frekuensi relaksasi dari mode Goldstone antiferroelektrik and 'mode frekuensi rendah' berkurang seiring dengan naiknya temperatur sehingga mencapai bagian tengah dari fasa smektik-C_α*.

Kata kunci : Kristal cair antiferroelektrik, konstanta dielektrik nonlinier, MHPOCBC, mode relaksasi

INTRODUCTION

The chiral smectic-C_α* (SmC_α*) phase has been the characteristic feature of several antiferroelectric liquid crystal compounds. Since this phase was reported in the 4-(1-methyl-heptyloxycarbonyl) phenyl 4-octylbiphenyl-4-carboxylate (MHPOBC), then the structure and physical properties have been studied extensively. According to the recent resonant x-ray scattering [1-3] and optical experimental results [4-6], the molecules in the SmC_α* phase are tilted with respect to the layer normal and the tilt direction is modulated incommensurately along the layer normal. The modulation period was shown to vary in few layers with decreasing the temperature.

Before the above experiments were performed, Cepic *et. al.* [7] has proposed a simple discrete phenomenological model, where the energy expansion in terms of order parameter takes into account interactions between the nearest and the next nearest smectic layer. By minimizing the free energy of the system, the short-period structure of the SmC_α* phase was obtained. Then, they studied theoretically the dynamic properties of SmA- SmC_α* phase transition in which competing interlayer interactions play an important role [8]. The SmA-SmC_α* phase transition is a second order and considered to be brought about by condensation of overdamped collective orientational soft modes. The soft mode is thought to be a helically tilted mode with a short pitch, and it exists at a general point of the smectic Brillouin zone in the SmA phase. In the tilted SmC_α* phase the soft mode splits into two modes, i.e. a phase and an amplitude mode. The existence of the soft mode is necessary for this scenario of the phase transition.

The dynamics in the vicinity of SmA-SmC_α* phase transition has been investigated by linear dielectric measurement and its dc bias effect [9-14], dynamic light scattering [15,16], and electro-optical measurement [17]. From some of these results, the ferroelectric mode was found in SmA and SmC_α* phases, and also the amplitude mode in SmC_α* phase close to SmA phase. In the SmC_α* phase the observation of the amplitude mode is not so difficult because the mode is located at the Brillouin zone center While in the SmA phase the soft mode is located at a

general point of the Brillouin zone and therefore it is difficult to observe this mode.

The response of dielectrics to an external field have been extensively used in order to clarify the phenomena related to the structural phase transition in ferroelectric and antiferroelectric liquid crystals. However, the investigation has been mainly confined to a linear response, which is proportional to the applied field, i.e. a linear dielectric measurement. It can detect only modes which induce macroscopic polarization such as the ferroelectric (soft) and Goldstone modes. On the other hand, the phase transition usually take place with the effect of nonlinearity, and so we believe to understand the phase transitions, the nonlinear nature in the materials of our interest has to be studied more. Moreover, the nonlinear dielectric constant ε_n ($n > 1$) of liquid crystals is large in general than that of crystals. The measurement of dielectric constant, therefore, can be extended to the higher harmonic responses and this nonlinear dielectric measurement is expected to give more detailed information about the orientational fluctuation in liquid crystals which can not be observed by the linear one.

Recently, we have performed the simultaneous linear and third-order nonlinear dielectric measurement to investigate in detailed the dynamic properties in the vicinity of the SmA- SmC_α* phase transition of an antiferroelectric liquid crystal MHPOCBC compound [18,19]. A Landau-type theory was developed to analyze the frequency dispersions of the third-order responses. By utilizing the theory we observed the amplitude mode in SmC_α* phase. We have also succeeded in obtaining the relaxation frequency of the soft mode in the SmA phase by taking advantage of the large fluctuations inducing the third-order nonlinear response. The relaxation frequency critically slows down as we approach the phase transition point obeying the Curie-Weiss law. This result is therefore a direct evidence that the SmA- SmC_α* phase transition is brought about by the soft mode condensation of an overdamped-collective mode. Then in SmC_α* phase close to SmA phase, the relaxation frequency of amplitude mode increases with the decreasing temperature in slope about four times compare with soft mode, indicating that this phase transition is close to a tricritical point [19]. We emphasize here that the nonlinear dielectric spectroscopy has an outstanding merit that we can measure the frequency dispersion of soft mode with non-zero wave numbers by means of it.

We have observed in detailed the dynamics in the vicinity of SmA-SmC_α* phase transition. Meanwhile, in the low temperature region of SmC_α* phase in MHPOCBC compound, it is observed that the frequency dispersion of the linear dielectric constant is strongly influenced by an applied dc field than in the high-temperature region near the SmA phase [11], and a mode in low frequency region was also found under applying dc-bias field in addition to the ferroelectric mode [10]. But there is no detailed report in describing the dynamic properties in this low temperature region. In this paper, we performed the detailed the linear and third-order nonlinear spectroscopy measurement and their dc bias effect, especially in the low temperature region of SmC_α* phase in order to give a deep insight about dynamic properties in this phase.

EXPERIMENTAL METHOD

The sample used in the present experiment was 4-(1-methyl-heptyloxycarbonyl)phenyl 4-octylcarbonyloxybiphenyl-4-carboxylate (MHPOCBC), the phase sequence of which is Cryst - SmI_A* - SmC_A* - SmC_a* - SmA- Iso [20]. This liquid crystal is a unique compound which has a direct phase transition from intermediate SmC_a* phase to antiferroelectric SmC_A* phase while in the other compounds have ferroelectric and ferrielectric phases, in addition to the large temperature interval of SmC_α* phase. The investigations presented here all have been performed in commercially available EHC cells with a cell gap of 12 and 25 μm, the area of electrodes was 4x4 mm^2, and a unidirectionally rubbed polyimide coating for planar alignment. The sample was introduced into a cell in the isotropic phase and cooled down slowly to the SmA phase. To achieve homogeneous alignment we applied a triangular wave of 15 V/μm at frequency 15 Hz, and performing several cooling-heating cycles over the SmA - SmC_α* phase transition.

The complex linear dielectric constants without and under dc-biased field were calculated from the capacitance and dielectric loss measured by an impedance analyzer (Hewlett-Packard, HP4194A). The driving AC electric field was kept as low as 4 mV/μm to avoid nonlinear effects on the dielectric constant, and a dc biased voltage up to 35 V was applied while performing the dc bias effect measurement. The linear dielectric measurements was performed used the homogeneous cell with the thickness 12 μm as follows. After stabilizing the temperature, the real and the imaginary parts of the dielectric constants, ε' and ε" were measured in the frequency range between 100 Hz and 10 MHz. In the measurement under a certain biased field, in order to avoid the free-charge accumulation due to the applying of the dc biased field, the reverse biased field was applied for the same period after each measurement. The measurements were repeated at increments of 0.1°C. In analysis, we fitted the frequency dispersion using the least square method to the Cole-Cole expression,

$$\varepsilon_1(\omega) = \varepsilon_\infty + \sum_{j=1}^{n} \frac{\Delta\varepsilon_j}{1+\left(i\omega\tau_{r,j}\right)^{\beta_j}} + \frac{1}{\left(i\omega\tau_c\right)^{\delta}} \quad \text{..... (1)}$$

where the last term has been added to take into account the conductivity of the samples which appeared at the

Vol. 7, No. 3, Juni 2006, hal : 18 - 25
ISSN : 1411-1098

low frequency, ε_∞ is the dielectric constant at the high frequency limit, and τ_{rj}, $\Delta\varepsilon_j$ and β_j are the relaxation time, the dielectric strength and the distribution parameters for the *j*-th mode, respectively.

Regarding nonlinear experiments, there is no devices commercially available for measurements of the nonlinear dielectric constants at various frequencies. Moreover, in general, the nonlinear response is much smaller than the linear one and so its precise measurement is difficult. The measurement system has been described in detailed in our previous paper [19]. This system utilizes the vector signal analyzer (HP89410A) which allow us to obtain the amplitudes and the phases of the linear and the third-order dielectric responses, simultaneously. The 25 mm cell was mounted in a hot stage (Instec HS1). The frequency dispersions in all phases of the samples were measured from 10 Hz to 1 MHz at stabilized temperatures on cooling process with a step of 0.1°C.

Nonlinear dielectric constants are defined as follows. When a cosine electric field with amplitude E_0 and frequency w, $E=E_0 \cos \omega t$, is applied to the materials with the center of symmetry, the electric displacement *D* can be expressed in terms of linear and nonlinear dielectric constants as,

$$D = \left\{ \varepsilon_1(\omega)\left(\frac{E_0}{2}\right) + 3\varepsilon_3(\omega)\left(\frac{E_0}{2}\right)^3 + \ldots \right\} e^{i\omega t} + \left\{ \varepsilon_3(\omega)\left(\frac{E_0}{2}\right)^3 + 5\varepsilon_5(\omega)\left(\frac{E_0}{2}\right)^5 + \ldots \right\} e^{i3\omega t} + \ldots + c.c. \quad \ldots\ldots (2)$$

where $\varepsilon_1(\omega)$ is the linear dielectric constant and the other coefficients are nonlinear dielectric constants. We have assumed that the sample is nonpolar, and from the reason of symmetry no eventh-order terms with respect to the field strength should appear. In fact, the second-order harmonic was confirmed, within experimental error, not to exist. In the present experiments we measured the linear dielectric constant $\varepsilon_1(\omega)$ and the third-order dielectric constant $\varepsilon_3(\omega)$. From eq. (2) it is clear that in the actual measurements it is necessary to check the linearity between the *n*th-order response D_n and E_0^n in order to obtain $\varepsilon_n(\omega)$. Otherwise, the higher-order contributions are included and the correct value cannot be obtained.

RESULTS AND DISCUSSION

Temperature Hysteresis of Linear Dielectric Constant

The temperature dependences of the real part of the linear dielectric constants in cooling and heating processes of MHPOCBC compound are shown in Figure 1, measured at 1 kHz with thickness 12 μm cell without applying dc-field. Three temperature regions are clearly recognized, which correspond to paraelectric SmA, SmC_α* and antiferroelectric SmC_A* phases with decreasing temperature, respectively.The transition temperature between the SmA and SmC_α* phases is identified by the peak of the linear dielectric constant, which have been confirmed by performing a detailed simultaneous dielectric and dc-signal of electro-optical measurement [21]. The transition to the SmC_A* phase is recognized as a steep decreasing in the linear dielectric constant value at low temperatures.

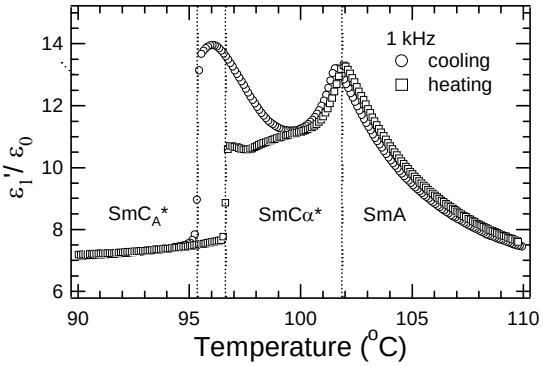

Figure 1. Temperature dependences of the real parts of $\varepsilon_1(\omega)$ measured on cooling and heating process with the rate of 0.1°C/min and the frequency of 1 kHz

These transition points are also determined from the break points on the temperature-dependence of frequency relaxation f_r of ferroelectric mode as shown in Figure 2. Around the SmA- SmC_α* phase transition, the dielectric constants of both processes cooling and heating are nearly coincide, while in the SmC_α*- SmC_A* phase transition we observe the hysteresis behavior of phase transition temperature. These results give the evidence that the higher temperature phase transition is a second-order, whereas the lower one is first-order phase transition as well as the continuity of the dielectric constant value in high temperature and the jump of it in the low temperature.

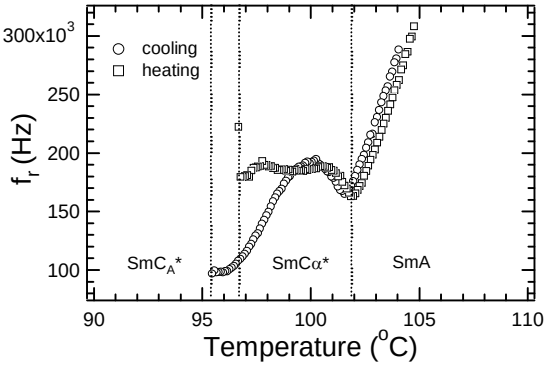

Figure 2. Temperature dependences of the relaxation frequency of ferroelectric mode obtained from the fitting result of the linear dielectric frequency dispersion by using Eq. (1), where n=1 and $f_r = 1/2\pi\tau_r$ measured on cooling and heating process

An interesting feature seen in this figure is the hysteresis of the linear dielectric constant in the low

temperature region of the SmC_α* phase. The value in the cooling process is larger than that of the heating process. This hysteresis of dielectric constant with temperature in the SmC_α* phase is also obtained within different thickness of samples and observed in other several compounds [22]. As shown in figure 2, we also obtained the hysteresis behavior on the temperature dependence of relaxation frequency of ferroelectric mode which has involved in the frequency dispersion. According to the recent helical pitch measurement in MHPOCBC by means differential optical reflectivity method, with the decreasing of temperature the helical pitch in SmC_α* phase decreases within few layer structures, then in the heating measurement no hysteresis of pitch change was observed [23]. This experiment used the homeotropic cell, therefore with temperature change, the helical pitch may change freely. While in the dielectric measurement, we used homogeneous cell where the helical pitch is suppressed and difficult to change due to surface anchoring, and the change of the pitch occured by generation and disappearance of phase defect. We suggest that the hysteresis of dielectric constant in low temperature region related to the changing of this pitch. In the cooling process measurement, the pitch become shorter accompanied by the generation of defect. In the heating process, the change of pitch to be longer accompanied with the disappearance of defect, and the influence of the short pitch in low temperature region is still remain. Therefore, there is a different mobilities of the generation and disappearance of defects related to the changing of the helical pitch in cooling and heating process. This is the origin of hysteresis. While in the high temperature region, since the tilt angle of liquid crystal molecule is small, the generation and disappearance of defect easily occur then no hysteresis observed.

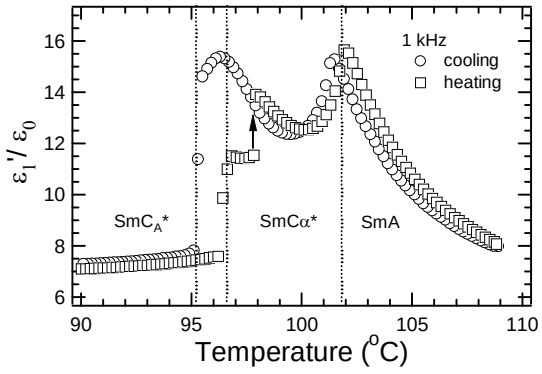

Figure 3. Temperature dependences of the real parts of $\varepsilon_1(\omega)$ measured on cooling and heating process with the rate of 0.1°C/min and the frequency of 1 kHz. In the low temperature region of SmC_α* phase we applied the dc-bias field on the heating process.

In order to verify this explanation we performed the linear dielectric constant measurement as follows. After performing the cooling measurement from SmA to SmC_A* phase, we made the measurement at heating process from SmC_A* phase, and in the low temperature region of SmC_α* phase we stop the measurement and then applied the dc-field to the sample which quiet high to unwound the helical structure. After switch off the field, we continue the measurement in heating process as the result is shown in figure 3, indicated by the arrow. As seen in the figure 3, the result after applying dc-field has the same behavior with the measurement in cooling process. We can explain this result as follows. By applying the quiet high dc-field, the helical structure will be unwound or the pitch become longer, and when switch off the field and make the heating measurement, it will be same with making the measurement in cooling where the pitch changes from the longer condition to the shorter condition. This results proved our idea that the hysteresis related to the change of helical pitch.

Linear and Nonlinear Dielectric Measurement

In order to observe the dynamic properties in SmC_α* phase, we also carried out the simultaneous measurement of frequency dispersion of the linear and the third-order dielectric constant. Figure 4 shows the temperature dependences of the real part of the linear and the third-order dielectric constants measured at 1 kHz with thickness 25 μm cell without applying dc-field in cooling process. Before continuing analyze the results, we focus our attention to the linear dielectric constant by comparing the results with figure 1 which has different cell gap. We obtained no significant change of dielectric constant in the high temperature region around SmA-SmC_α* phase transition, while in the low temperature region, the peak of linear dielectric constant shifted to the lower temperature as decreasing the thickness. These results indicated that the low temperature region of SmC_α* phase of MHPOCBC is strongly affected by surface anchoring as mentioned before.

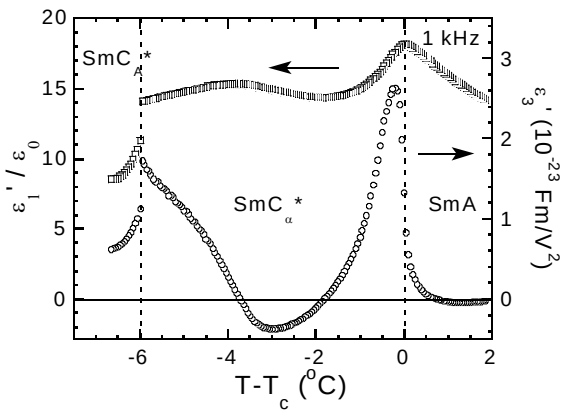

Figure 4. Temperature dependences of the real parts of $\varepsilon_1(\omega)$ and $\varepsilon_3(\omega)$ measured simultaneously at 1 kHz on cooling process with the rate of 0.1°C/min and the frequency of 1 kHz. The abscissa is a temperature difference from the SmA-SmC_α* phase transition temperature.

Vol. 7, No. 3, Juni 2006, hal : 18 - 25
ISSN : 1411-1098

In Figure 4, third-order nonlinear dielectric constant shows a complicated temperature dependence behavior in SmA and SmC_α* phase. At high temperatures far from the transition point in the SmA phase the real part is negative and increases with decreasing temperature and then it becomes zero above the transition point to change the sign positive. In the vicinity of the transition point it increases steeply and takes a sharp peak below the transition temperature in SmC_α* phase. Orihara *et. al*. have succeeded to explain the anomalous behavior in this phase by a theory that takes into account the pretransitional fluctuation [24]. In SmC_α* phase, with decreasing the temperature, the third-order dielectric constant decreases as well as the linear one. Then about 2°C below the transition point, where the linear dielectric constant has a minima, the value become zero and change to negative. With decreasing temperature, it takes a peak in negative and then change the sign again to positive close the transition point to SmC_A* phase. We also observed the hysteresis of the third-order dielectric constant with temperature in the low temperature region while performing the measurement in heating process as well as the linear one.

Here, let us discuss the reason why the third-order nonlinear dielectric constant become negative in higher temperature region of SmC_α* phase as shown in Figure 4. As mentioned in our previous paper that there are two main contributions to the third-order dielectric constant in SmC_α* phase close to the SmA phase, amplitude mode and ferroelectric mode [19]. The former one takes positive value in the contribution and gradually decreases with decreasing temperature. The latter one takes negative value and slightly change with temperature. When the absolute values of this two terms coincide, the third-order dielectric constant vanishes. The negative value may be caused by the increasing of ferroelectric mode contribution, as we observed by the increasing of dielectric constant.

Figure 5 shows a tridimensional plot of the imaginary part of linear dielectric constant, ε_1", versus temperature and frequency of the applied field in the cooling process. It is seen that only one relaxation process is involved in the linear dielectric constant without dc-bias field in the measured frequency region throughout the temperature, i.e. n=1 in Eq. (1). The observed peak is corresponding to the relaxation frequency of the ferroelectric mode, a homogeneously tilting mode which induces the macroscopic polarization.

Figure 6 shows the frequency dispersions of the imaginary part of the third-order nonlinear dielectric constant on cooling process. From this figure we can observe one peak in higher temperature which was explained in our previous study [19]. The peak is corresponding to the relaxation frequency of the amplitude (soft) mode which induces the SmA-SmC_α* phase transition. In the SmC_α* phase, close to the higher phase transition, we observed the increasing of the relaxation frequency of amplitude mode with decreasing the temperature. In low temperature region close to the transition point to SmC_A* phase, we observed another peak, and continuously exist within the SmC_A* phase though the dielectric strength of the mode jump and become smaller. As mentioned in the other papers, the relaxation process obtained in SmC_A* phase by using the third order nonlinear dielectric constant measurement is due to the antiferroelectric Goldstone mode which are not able to obtained by the usual linear dielectric measurement [25,26]. Since the peak in SmC_A* phase with increasing temperature continously exist in the SmC_α*, we suggest that the mode become stronger in the low temperature region close to the transition point to SmC_A* phase is the antiferroelectric Goldstone mode. We also observed a small peak in the middle of SmC_α* phase at low frequency region. The relaxation process here is not the same with the higher temperature mode, since the dielectric strength of the amplitude mode in higher temperature becoming zero. We designated this mode as 'low frequency mode'. In order to understand the behavior of these modes, we should investigate the temperature dependence of the relaxation frequency of these modes. Since we have no expression for the third-order response in the low temperature region, we

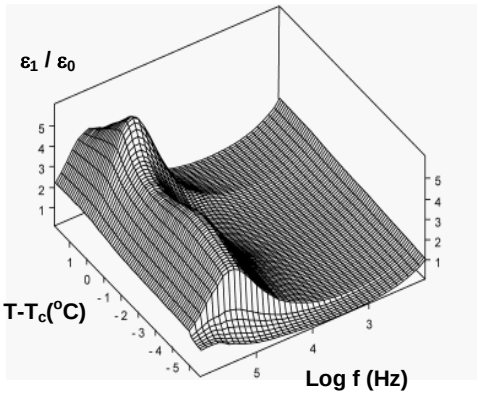

Figure 5. Temperature dependence of the imaginary part of the linear dielectric frequency dispersion in ε_1"(ω).

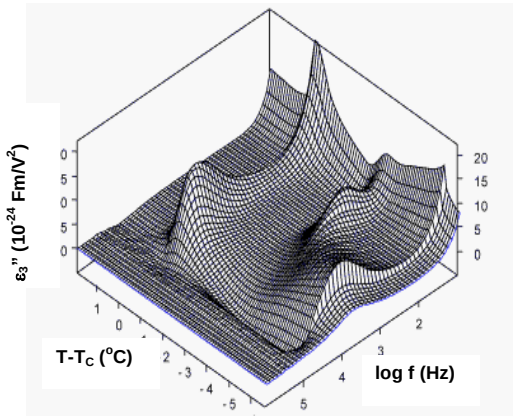

Figure 6. Temperature dependence of the imaginary part of the third-order nonlinear dielectric frequency dispersion in ε_1"(ω).

determine the relaxation frequency of the third-order dielectric constant from the peak of each imaginary part.

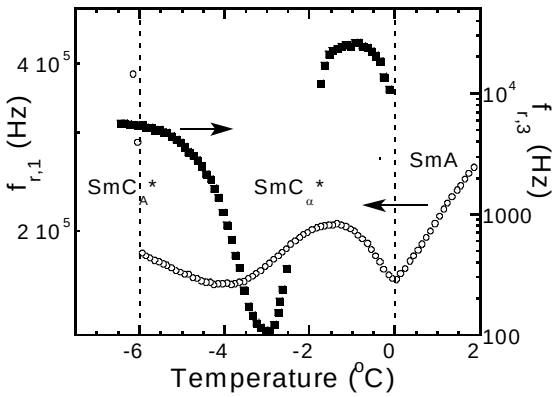

Figure 7. Temperature dependences of the relaxation frequencies of obtained from the linear and the third-order nonlinear dielectric spectroscopies. The relaxation frequency of ferroelectric mode, $f_{r,1}$, were obtained from the fitting results of the linear dielectric frequency dispersion by using Eq. (1), whereas for the low frequency mode, $f_{r,3}$, were determined from the peak value of the third-order nonlinear dielectric frequency dispersion.

Figure 7 shows the temperature dependences of the relaxation frequency obtained from the fitting results for the linear dielectric frequency dispersion and from the peak frequency for the third-order nonlinear frequency dispersion. The observed relaxation in the high frequency shown by the circle marks is due to a ferroelectric mode, which induces a macroscopic polarization. Around the SmA-SmC_α* phase transition, its relaxation frequency becomes soft in both phases as approach the transition point. In the SmC_α* phase, with the decreasing temperature, the relaxation frequency first increases,and then have the minima again whereas the dielectric strength made a maxima in low temperature region. In the SmC_A*- SmC_α* phase transition the relaxation frequency shows the jump and become much higher SmC_A* phase just after the phase transition than the measuring region.

The relaxation frequency in the higher frequency region of SmC_α* phase have been discussed in detailed in our previous paper [19], we will discuss about this. The lower frequency relaxation in the low temperature region of SmC_α* phase is due to antiferroelectric Goldstone mode and low frequency mode. We can observe that the relaxation frequency of both modes change continuously thus we can not distinguish them, it may be the same mode though the dielectric strength of low frequency mode show a little peak before continuing. With increasing the temperature, we observe the softening of antiferroelectric Goldstone mode and low frequency mode. These results show that in the low temperature region of SmC_α* phase there is a different behavior under field to without electric field measurement. Without applied field, with decreasing temperature the whole SmC_α* phase consists of one phase since there is no significant change observed as shown by DSC [20], birefringence, tilt angle [27] and helical pitch [23] measurements.

Linear Dielectric Measurements Under DC Field

In order to investigate the detailed behavior of low temperature region, we carried out the linear dielectric constant measurements under dc field which causes the structural change of the sample. Figure 8 shows the temperature and dc-bias field dependences of the real part of the linear dielectric constant, ε_1', measured at 1 kHz on cooling process. We can obtain the electric field (E) - temperature (T) phase diagram of SmA, SmC_α* and SmC_A* phases by looking down from the top of the Figure 8 as shown with contour graph in Figure 9. The similar E-T phase diagram was obtained before by Hiraoka *et. al.* utilizing the apparent tilt angle measurements [10]. Recently, we also performed the simultaneous birefringence and tilt angle measurements, and obtained more detailed E-T phase diagrams of MHPOCBC [28]

In high temperature, without dc-field, we can see

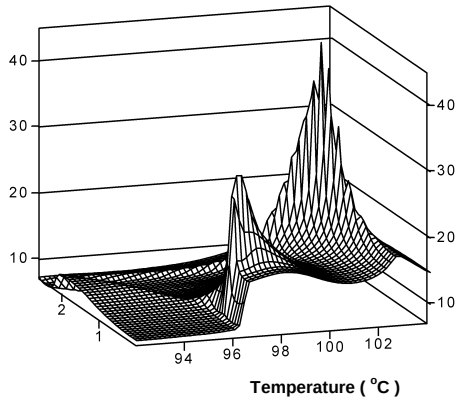

Figure 8. Dc-bias field dependences of the linear dielectric constant. .....gambar dibetulkan

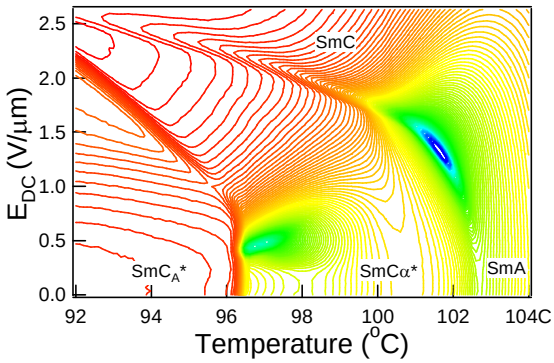

Figure 9. The contour graph of E-T phase of MHPOCBC obtained from the Figure 8.

Vol. 7, No. 3, Juni 2006, hal : 18 - 25
ISSN : 1411-1098

that ε_1' make a peak indicating the SmA- SmC_α* phase transition. The peak value increases as increasing the dc-field, and shift to the lower temperature. After ε_1' has a maximum, the peak values become smaller. The maximum peak related to the field-induced tricritical point where the second order phase transition change to the first order with increasing dc-bias field, and dielectric constant theoretically become divergence in this point. Bourny and Orihara also confirmed in detailed the existence of this critical point theoretically and experimentally with several measurements [29]. In the low temperature region, we observed the dielectric constant anomaly due to the structural change related to the unwound process of helical structures. SmC_α* phase changes into a field-induced intermediate phase under a weak applied dc-field before the phase transition to the SmC phase occurs. It is different from the higher temperature behavior which shows the direct phase transition between two phases. According to the conoscope observation [30], this intermediate phase shows *ferrielectriclike* response very similar to the SmC_γ* phase of MHPOBC [31].

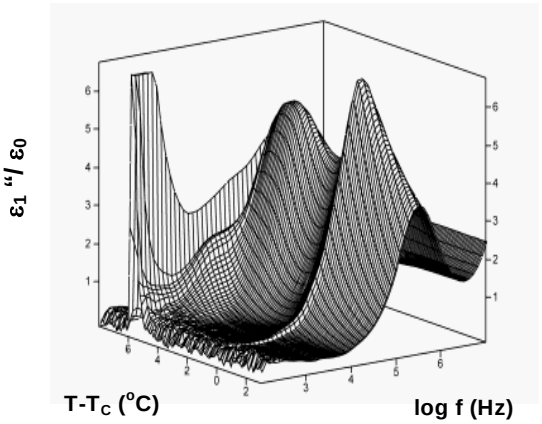

Figure 10. Temperature dependence of the imaginary part of the linear dielectric frequency dispersion in e_1"(w) under DC-bias field.

In Figure 10, the temperature dependences of the imaginary part of the dielectric constant, ε_1", for dc-bias field 0.36 V/μm is presented in order to show the dynamic behavior under dc-biased field. The bias value is quiet small under the value where the structural change occured in the low temperature region of SmC_α* phase. As well as the results for dc-bias field zero, we observed the relaxation process due to the ferroelectric mode in the high frequency region in all temperatures.

It is important to notice that in the low temperature region of SmC_α* phase, a new mode appears in the low frequency region. This mode can be observed also at weaker electric fields, though the relaxation strength is small. At the transition point to the SmC_A* phase a steep increase of dielectric constant value was observed. This should be due to the coexistence of both SmC_a* and SmC_A* phases as usually seen at a first-order phase order transition. The frequency dispersions were analyzed in terms of the Cole-Cole formula in Eq. (1), and since another mode was necessary for the fitting, we put n=2 in above equation.

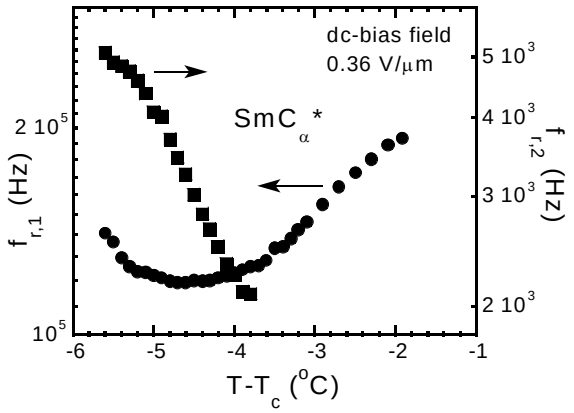

Figure 11. Temperature dependences of the relaxation frequencies obtained from the linear dielectric frequency dispersion under dc-bias field in the low temperature region of the SmC_a* phase.

Figure 11 shows the temperature dependences of relaxation frequencies obtained from the frequency dispersion under dc-bias field 0.36 V/μm. The high frequency mode, ferroelectric mode shows the same behavior as well as the results without no bias field. In the low temperature region we observed the relaxation frequency of the low frequency mode decreases with increasing temperature, though we only observe this softening in a narrow temperature interval since the relaxation strength becoming very small. This results was in a good agreement with the softening of the mode obtained from the third-order nonlinear dielectric constant. Therefore, we suggest that the new mode obtained in the two measurements has the same origin, i.e. Goldstone mode. But in the linear dielectric constant measurement under dc-field, we can not observed the decreasing of relaxation frequency of 'low frequency mode' in higher temperature as it has been investigated by the third-order nonlinear dielectric measurement.

CONCLUSIONS

We have performed the linear dielectric constant measurement in cooling and heating process within the SmC_α* phase of MHPOCBC. It is obtained that the thermal hysteresis of dielectric constant can be observed at low temperature region of SmC_α* phase due to the changing of helical pitch induced by the generation and disappearance of defects. From the simultaneous measurement of linear and third-order nonlinear dielectric spectroscopies in the low temperature region of the SmC_α* phase of antiferroelectric liquid crystal MHPOCBC, we observed the softening of the Goldstone mode and low frequency mode with increasing the temperature. The existence of Goldstone mode was

confirmed by means of the linear dielectric measurement under dc-bias field.

ACKNOWLEDGMENTS

We would like to thank Showa Shell Sekiyu Co. Ltd. for supplying MHPOCBC.

REFERENCES

[1]. P. MACH, R. PINDAK, A.M. LEVELUT, P. BAROIS, H.T. NGUYEN, C.C. HUANG, and L. FURENLID, *Phys. Rev. Lett.*, **81** (1998) 1015

[2]. P. MACH, R. PINDAK, A.M. LEVELUT, P. BAROIS, H.T. NGUYEN, H. BALTES, M. HIRD, K. TOYNE, A. SEED, J. W. GOODBY, C. C. HUANG, and L. FURENLID, *Phys. Rev. E*, **60** (1999) 6793

[3]. L. S. HIRST, S. J. WATSON, H. F. GLEESON, P. CLUZEAU, P. BAROIS, R. PINDAK, J. PITNEY, A. CADY, P. M. JOHNSON, C. C. HUANG, A.-M. LEVELUT, G. SRAJER, J. POLLMANN, W. CALIEBE, A. SEED, M. R. HERBERT, J. W. GOODBY, and M. HIRD, *Phys. Rev. E*, **65** (2002) 041705

[4]. D. SCHLAUF, CH. BAHR, AND H.T. NGUYEN, *Phys. Rev. E*, **60** (1999) 6816

[5]. P. M. JOHNSON, S. PANKRATZ, P. MACH, H. T. NGUYEN, and C.C. HUANG, *Phys. Rev. Lett.*, **83** (1999) 4073

[6]. D. A. OLSON, S. PANKRATZ, P. M. JOHNSON, A. CADY, H. T. NGUYEN, and C. C. HUANG, *Phys. Rev. E*, **63** (2001) 061711

[7]. M. CEPIC and B. ZEKS, *Mol. Cryst. Liq. Cryst.Sci. Technol. Sect. A*, **263** (1995) 61

[8]. M. CEPIC and B. ZEKS, *Liq. Cryst.*, **20** (1996) 29

[9]. M. FUKUI, H. ORIHARA, A. SUZUKI, Y. ISHIBASHI, Y. YAMADA, N. YAMAMOTO, K. MORI, K. NAKAMURA, Y. SUZUKI, and I. KAWAMURA, *Jpn. J. Appl. Phys.*, **29** (1990) L329

[10]. K. HIRAOKA, Y. TAKANISHI, H. TAKEZOE, A. FUKUDA, T. ISOZAKI, Y. SUZUKI, and I. KAWAMURA, *Jpn. J. Appl. Phys.*, **31** (1992) 3394

[11]. M. CEPIC, G. HEPPKE, J.-M. HOLLEDT, D.L. HOTZSCH, D. MORO, and B. ZEKS, *Mol. Cryst. Liq. Cryst.Sci. Technol. Sect. A*, **263** (1995) 207

[12]. S. SARMENTO, P. S CARVALHO, M. R. CHAVES, H.T. NGUYEN and F. PINTO, *Mol. Cryst. Liq. Cryst.Sci. Technol. Sect. A*, **328** (1999) 457

[13]. R. DOUALI, C. LEGRAND, V. FAYE, and H.T. NGUYEN, *Mol. Cryst. Liq. Cryst.Sci. Technol. Sect. A*, **328** (1999) 209 ; R. DOUALI, C. LEGRAND, and H.T. NGUYEN, *Ferroelectrics*, **245** (2000) 101

[14]. V. BOURNY and H. ORIHARA, *Phys. Rev. E*, **63** (2001) 21703

[15]. D. KONOVALOV and S. SPRUNT, *Phys. Rev. E*, **58** (1998) 6869

[16]. A. RASTEGAR, TH. RASING, I. MUSEVIC, and G. HEPPKE, *Phys. Rev. E*, **60** (1999) 6788

[17]. V. BOURNY, A. FAJAR, and H. ORIHARA, *Phys. Rev. E*, **62** (2000) R5903

[18]. H. ORIHARA, A. FAJAR, and V. BOURNY, *Phys. Rev. E*, **65** (2002) 040701

[19]. A. FAJAR, H. MURAI, and H. ORIHARA, *Phys. Rev. E*, **65** (2002) 041704

[20]. T. ISOZAKI, Y. SUZUKI, I. KAWAMURA, K. MORI, N. NAKAMURA, N. YAMAMOTO, Y. YAMADA, H. ORIHARA, and Y. ISHIBASHI, *Jpn. J. Appl. Phys.*, **30** (1991) L1573.

[21]. A. FAJAR, Doctoral Thesis, Nagoya University, (2003)

[22]. H. TAKEZOE, K. HIRAOKA, T. ISOZAKI, K. MIYACHI, H. AOKI, and A. FUKUDA, *Modern Topics in Liquid Crystals - From Neutron Scattering to Ferroelectricity*, ed. A. Buka, World Scientific, Singapore, (1993)

[23]. A. CADY, D.A. OLSON, X.F. HAN, H.T. NGUYEN, H. ORIHARA, and C.C. HUANG, *unpublished*

[24]. H. MURAI, V. BOURNY, A. FAJAR, and H. ORIHARA, *Mol. Cryst. Liq. Cryst.Sci. Technol. Sect. A*, **366** (2001) 645.

[25]. H. ORIHARA and Y. ISHIBASHI, *J. Phys. Soc. Jpn.*, **64** (1995) 3775

[26]. K. OBAYASHI, H. ORIHARA, and Y. ISHIBASHI, *J. Phys. Soc. Jpn.*, **64** (1995) 3118

[27]. M. SKARABOT, M. CEPIC, B. ZEKS, R. BLINC, G. HEPPKE, A.V. KITYK, and I. MUSEVIC, *Phys. Rev. E*, **58** (1998) 575.

[28]. H. ORIHARA, Y. NARUSE, M. YAGYU, A. FAJAR, AND S. UTO : *Phys. Rev. E*, **72** (2005) 040701

[29]. V. BOURNY and H. ORIHARA, *Phys. Rev. E*, **63** (2001) 21703

[30]. T. ISOZAKI, K. HIRAOKA, Y. TAKANISHI, H. TAKEZOE, A. FUKUDA, Y. SUZUKI, and I. KAWAMURA, *Liq. Cryst.*, **12** (1992) 59

[31]. E. GORECKA, A.D.L. CHANDANI, Y. OUCHI, H. TAKEZOE, and A. FUKUDA, *Jpn. J. Appl. Phys.*, **29** (1990) 131